

Probing long-period companions to planetary hosts

VLT and CFHT near infrared coronagraphic imaging surveys

G. Chauvin¹, A.-M. Lagrange², S. Udry³, T. Fusco⁴, F. Galland², D. Naef¹, J.-L. Beuzit², and M. Mayor³

¹European Southern Observatory, Casilla 19001, Santiago 19, Chile

²Laboratoire d'Astrophysique, Observatoire de Grenoble, 414, Rue de la piscine, Saint-Martin d'Hères, France

³Observatoire de Genève, 51 Ch. des Maillettes, 1290 Sauverny, Switzerland

⁴ONERA, BP52, 29 Avenue de la Division Leclerc Châtillon Cedex, France

Received; accepted

ABSTRACT

Aims. We present the results of a deep imaging survey of stars surrounded by planets detected with the radial velocity technique. The purpose is to search for and to characterize long-period stellar and substellar companions. The sample contains a total of 26 stars, among which 6 exhibit additional radial velocity drifts.

Methods. We used NACO, at the ESO Very Large Telescope, and PUEO-KIR, at the Candian French Hawaiian Telescope, to conduct a near-infrared coronagraphic survey with adaptive optics of the faint circumstellar environment of the planetary hosts. The domain investigated ranges between 0.1'' to 15'' (i.e. about 3 to 500 AU, according to the mean distance of the sample). The survey is sensitive to companions within the stellar and the substellar domains, depending on the distance to the central stars and on the star properties.

Results. The images of 14 stars do not reveal any companions once the field objects are removed. 8 stars have close potential companions that need to be re-observed within 1–2 years to check for physical companionship. 4 stars are surrounded by faint objects which are confirmed or very probable companions. The companion to HD 13445 (Gl 86) is already known. The HD 196885 star is a new close visual binary system with a high probability of being bound. The 2 newly discovered companions, HD 1237 B and HD 27442 B, share common proper motions with the central stars. Orbital motion is detected for HD 1237 B. HD 1237 B is likely a low-mass M star, located at 70 AU (projected distance) from the primary. HD 27442 B is most probably a white dwarf companion located at about 240 AU (projected distance).

Key words. Stars: low-mass, brown dwarfs, planetary systems – Instrumentation: adaptive optics

1. Introduction

Since the discovery of 51 Peg b (Mayor & Queloz 1995), more than 160 extrasolar giant planets (EGPs) have been found through radial velocity (RV) measurements. Their physical and orbital characteristics (mass, separation, eccentricity) have challenged the scenario of planetary formation. The observed properties of the period-mass distribution show tendencies that need to be explained (Udry et al. 2003). There is a lack of very light ($\leq 0.75 M_{\text{Jup}}$) planets at long (≥ 100 days) periods, which cannot be explained by the observational bias inherent to the RV technique. There is a lack of massive ($\geq 2 M_{\text{Jup}}$) planets with short (≤ 100 days) periods and a lack of brown dwarfs (BDs) at short (≤ 4 AU) separations, known as the so-called “BD desert”. Whether this BD desert extends to larger separations is presently unknown. The present multiplicity studies

in the substellar domain are limited by small statistical samples (Gizis et al. 2001, McCarthy & Zuckerman 2004).

To understand the way(s) EGPs and BDs form and evolve, observational studies of their physical and orbital characteristics must be extended to longer periods and to lower masses. In addition, if EGPs or BDs are orbiting at large separations, they will gravitationally affect the formation and dynamical evolution of any possible inner planets (see Rivera & Lissauer 2000, Eggenberger et al. 2004). In particular, they will constrain the stability domain of the inner planetary system and may be responsible for the large eccentricities observed for several planets detected with the RV technique.

Up to now, the best method to detect close (≤ 4 AU) substellar companions has been the RV technique. However, this method is currently insensitive to larger separations. With the development of high contrast and high angular resolution imaging, resulting from large telescopes equipped with adaptive optics (AO) and coupled to dedicated focal de-

Table 1. Sample of planetary hosts observed with PUEO-KIR at CFHT and with NACO at VLT. The main properties of the systems are summarized. The telescopes, the number of companion candidates detected and their status are given with the number of observing epochs for each system.

Name	Other Name	V (mag)	K (mag)	d (pc)	SpT	b ($^{\circ}$)	Telescope	Nb cand.	Epochs	Status	References
HD 1237	GJ 3021	6.7	4.86	17.6	G6V	-37.1	VLT	1	3	C	1a
HD 13445	Gl 86	6.17	4.13	10.9	K1V	-62.0	VLT	1	3	C	2a – 1b, 3b, 4b
HD 17051	iot Hor	5.4	4.14	17.2	G0V	-58.3	VLT	1	2	B	3a
HD 27442		4.4	1.75	18.2	K2IV	-42.1	VLT	1	3	C	4a
HD 28185		7.81	6.19	39.6	G5	-36.0	VLT	0	1	N	5a
HD 52265		6.3	4.95	28.1	G0III-IV	-0.5	VLT	7	2	B	6a
HD 89744		5.74	4.45	39.0	F7V	+56.4	CFHT	1	1	U	7a
HD 92788		7.1	5.72	32.3	G5	+47.4	CFHT	0	1	N	8a
HD 95128	47 Uma	5.10	3.75	14.1	G1V	+63.4	CFHT	0	1	N	9a, 10a
HD 106252		7.36	5.93	37.4	G0V	+70.7	CFHT	0	1	N	11a
HD 114762		7.30	5.81	40.1	F9V	+79.3	CFHT	1	1	U	12a
HD 121504		7.6	6.12	44.4	G2V	+5.7	VLT	56	1	U	13a
HD 130322		8.05	6.23	29.7	K0III	+51.0	CFHT/VLT	1	2	B	14a
HD 141937		7.25	5.76	33.5	G2/G3V	+26.8	CFHT	1	1	U	15a – 2b
HD 154857		7.25	5.51	68.5	G5V	-10.0	VLT	28	1	U	16a
HD 160691	μ Arae	5.2	3.68	15.3	G3IV-V	-11.5	VLT	5	3	B	16a, 17a, 18a
HD 162020		9.18	6.54	31.2	K2V	-6.7	VLT	> 100	1	U	19a
HD 168443		6.92	5.21	37.9	G5	+2.5	CFHT	> 100 (5)	1	U (B)	19a – 2b
HD 179949		6.25	4.94	27.0	F8V	-15.8	CFHT	5	1	U	21a
HD 183263		7.86	6.42	52.7	G2IV	-4.3	VLT	57	1	U	22a
HD 186427	16 Cyg B	6.20	4.65	21.4	G3V	+13.2	CFHT	0	1	N	23a – 2b
HD 187123		7.86	6.34	47.9	G5	+4.7	CFHT/VLT	5	2	B	24a – 2b
HD 192263		8.1	5.54	19.9	K2V	-18.7	VLT	8	3	B	25a
HD 196885		6.4	5.07	33	F8IV	-18.0	VLT	3	1	U	no reference, 26a
HD 202206		8.1	6.49	46.3	G6V	-40.5	VLT	3	2	B	19a, 20a
HD 217107		6.2	4.54	19.7	G*IV	-53.3	VLT	0	1	N	27a

- RADIAL VELOCITIES REFERENCES: (1a) Naef et al. 2001, (2a) Queloz et al. 2000, (3a) Kurster et al. 2000, (4a) Butler et al. 2001, (5a) Santos et al. 2001, (6a) Butler et al. 2000, (7a) Korzennik et al. 2000, (8a) Fischer et al. 2000, (9a) Butler & Marcy (1996), (10a) Fischer et al. (2002a), (11a) Fischer et al. (2002b), (12a) Latham et al. (1989), (13a) Mayor et al. 2004, (14a) Udry et al. 2000, (15a) Udry et al. 2002, (16a) McCarthy et al. 2004, (17a) Butler et al. 2001, (18a) Santos et al. 2004, (19a) Udry et al. 2002, (20a) Correia et al. 2004, (21a) Tinney et al. 2000, (22a) Marcy et al. 2005, (23a) Cochran et al. 1997, (24a) Butler et al. 1998, (25a) Santos et al. 1999, (26a) <http://exoplanets.org/esp/hd196885/hd196885.shtml>, (27a) Fischer et al. 1999

- IMAGING REFERENCES: (1b) Els et al. 2001, (2b) Luhman & Jayawardhana 2002, (3b) Mugrauer & Neuhäuser 2005, (4b) Lagrange et al. 2006

- NOTES: (C) confirmed comoving object, (B) stationary background objects, (U) undefined sources and (N) no faint objects detected

vices, such as coronagraphs or differential imagers, BDs and very massive EGPs can now be rapidly probed at large separations (typically ≥ 50 –100 AU). Since the discovery of Gl 229 B (Nakajima et al. 1995), coronagraphic imaging techniques have been successfully used, from space and from the ground, to detect BD companions around nearby field stars: HR 7672 B (Liu et al. 2002), HD 130948 B (Potter et al. 2002), Gl 494 B (Beuzit et al. 2004), G 239-25 (Forveille et al. 2004) or, more recently, HD 49197 B (Metchev et al. 2004).

In order to push the detection performances down to the planetary mass regime, systematic searches have recently focused on young (1 – 50 Myr), nearby associations. EGPs and BDs are actually hotter, brighter and therefore easier to image when they are young. These surveys led to the detection of very low mass substellar companions of 10 to 30 M_{Jup} : HR 7329 B (Lowrance et al. 2000), TWA5 B (Lowrance et al. 1999), GSC 08047-00232 B (Chauvin et al. 2003) and, more recently AB Pic B (Chauvin et al. 2005). However, the most important results obtained so far are the discoveries of the possible plan-

etary mass companions to the young BD 2MASSWJ 1207334-393254 (Chauvin et al. 2004, 2005) and the young star GQ Lup (Neuhäuser et al. 2005).

In the context of older (0.5 – 10 Gyr) stars with planets detected through RV measurements, the detection capabilities are currently limited to massive BD companions. The discovery of the companion Gl 86 B (see Els et al. 2001) is a good illustration. Mugrauer & Neuhäuser (2005) have recently demonstrated that this object is likely to be a cool white dwarf, although its photometry is compatible with a T dwarf. In recent years, systematic searches of BDs orbiting planetary hosts have been conducted in the northern hemisphere (Oppenheimer et al. 2001, Luhman & Jayawardhana 2002, Patience et al. 2002). Of these, Luhman & Jayawardhana (2002) were the most sensitive one. However, none of the 25 stars that they observed revealed bound companions between a few tens and a few hundreds of AU of the primary.

In 2003, we commenced deep coronagraphic imaging survey of 26 planetary hosts, using PUEO-KIR, at CFHT, and

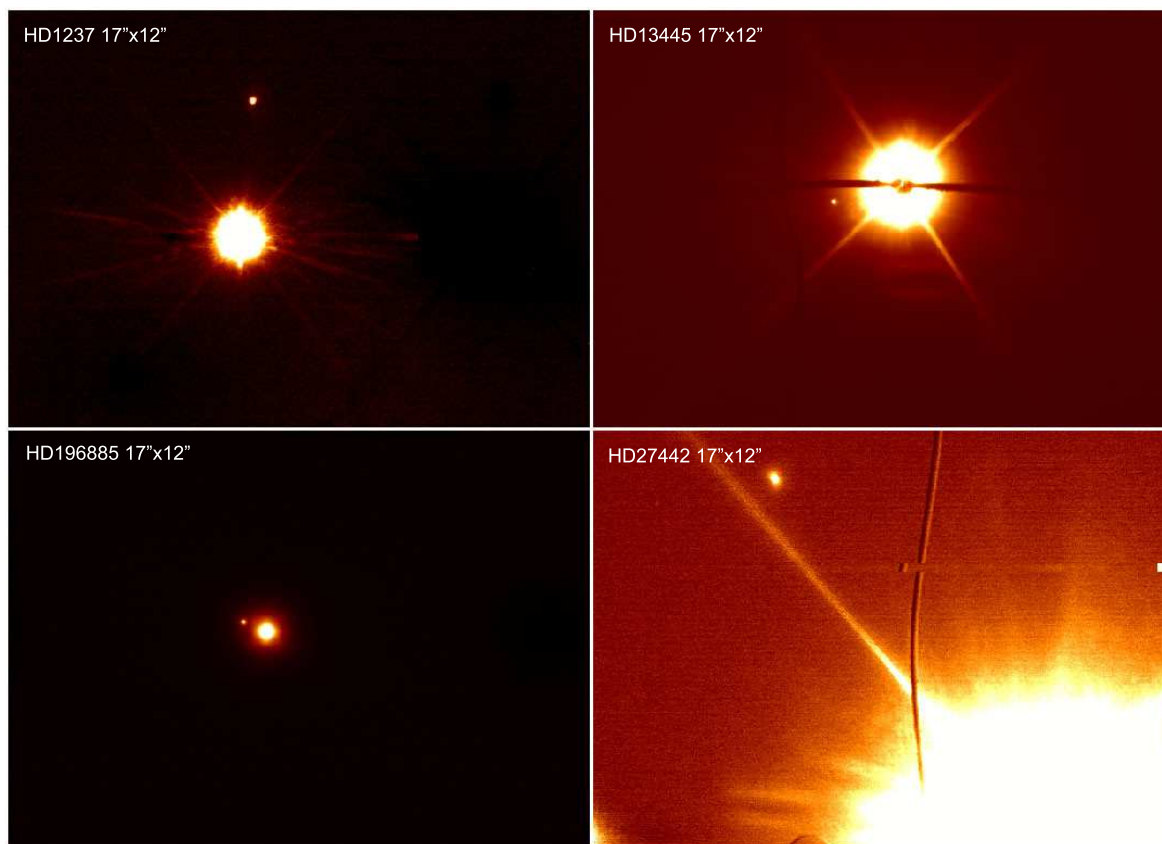


Fig. 1. VLT/NACO images of the companions to HD 1237, HD 13445 (Gl 86), HD 27442 and the very probable one to HD 196885. Orbital motion is detected for the companion to HD 13445 (Gl 86), known to be bound (Els et al. 2001, Mugrauer & Neuhäuser 2005, Lagrange et al. 2006). Follow-up observations indicate that the companion candidates HD 1237 and HD 27442 are comoving objects. We also detect the orbital motion of HD 1237 B relative to A, which confirms its companionship. Finally, HD 196885 is a close visual binary system with a high probability for being bound (see Section 4.2).

NACO, at VLT. We report in Section 2 the sample, observing strategy, instrument set-ups and the data reduction and analysis. We present in Section 3 the results of these observations and the detection performances achieved. Section 4 discusses in more detail those cases exhibiting RV drifts and for which no companions are known at long-periods. Finally, the discovery of the 2 companions to the stars HD 1237 and HD 27442, as well as the possible companion to the star HD 196885 is detailed.

2. Observations

2.1. Sample and observing strategy

Table 1 lists the main characteristics (distance, spectral type, VK magnitudes and galactic latitude) of the 26 stars observed. The observing strategy was similar at CFHT and at VLT. The first step was to obtain deep coronagraphic images to search for faint and close companion candidates in the circumstellar environment. Then, a non-saturated classical image was immediately recorded to obtain an accurate position of the star on the detector, to measure the relative photometry between the companion candidates and the star and to look for a very close binary. The detection survey was performed in K-band where

the AO correction is more reliable and the contrast between stars and substellar companions is optimal.

In cases of positive detection, the companion candidates were re-observed at a second epoch to check if the faint objects shared a common proper motion with the central star. Depending on the object proper motions, this required an interval of 1-2 years between successive observations. When true companions were detected, new images were also recorded in J and H bands for direct comparison with the photometry predicted by evolutionary models of stellar and substellar objects. Typical total exposure times were 5-10 minutes. However, only the highest quality exposures were retained, leading to an effective exposure time of about 5 minutes per target.

2.2. Instruments and astrometric calibration

2.2.1. PUEO-KIR at CFHT

The AO observations were carried out on May 20, 21 and 22 2003 at CFHT, using the 1024×1024 near-infrared camera KIR¹, coupled to the AO curvature system PUEO (see Roddier et al, 1991; Arsenaault et al, 1994) (located at the Cassegrain focus). We used the KIR upgrade coronagraphic mode (named

¹ <http://www.cfht.hawaii.edu/Instruments/Detectors/IR/KIR/>

Table 2. Detection performances of PUEO-KIR at CFHT and of NACO at VLT. The detection limits are converted in term of mass, based on the predictions of the BA98 (Baraffe et al. 1998) evolutionary model in the stellar regime and the COND03 (Baraffe et al. 2003) model in the substellar regime

Instrument	Separation (arcseconds)	ΔK (6σ) (mag)	M_K (6σ) (mag)	EVOLUTIONARY MODEL PREDICTIONS			
				Mass (0.5 Gyr) (M_{Jup})	Mass (1.0 Gyr) (M_{Jup})	Mass (5.0 Gyr) (M_{Jup})	Mass (10.0 Gyr) (M_{Jup})
CFHT/PUEO-KIR	1.0	8	10–12	70	75	80	80
	2.0	11	13–15	30	40	60	70
VLT/NACO	1.0	12	14–16	25	30	60	70
	2.0	13.5	16–18	15	20	40	50

GRIF) that provides an occulting mask with a diameter of $0.8''$. The coronagraphic observations were obtained with the K' ($\lambda = 2.12 \mu\text{m}$, $\Delta\lambda = 0.34 \mu\text{m}$) filter for all the CFHT sources. The direct imaging observations were obtained with the Bry ($\lambda = 2.166 \mu\text{m}$, $\Delta\lambda = 0.022 \mu\text{m}$) narrow band filter.

No astrometric calibrators were observed to properly determine the platescale and the detector orientation of the KIR camera. Therefore, we have used conservative values for the detector orientation and the platescale of respectively $0.0 \pm 2^\circ$ and $34.8 \pm 0.2 \text{ mas/pix}$. The total field of view (FoV) was then $35.6'' \times 35.6''$. Follow-up observations were done for only two stars (HD 130322 and HD 187123) with such significant proper motions that the companion candidates could be unambiguously identified as background objects.

2.2.2. NACO at VLT

The NACO observations were obtained during multipurpose runs of guaranteed time observations (GTO) and open time observations². The NACO³ instrument is equipped with an AO system (Rousset et al. 2002) that provides diffraction limited images in the near infrared (nIR) and illuminates the CONICA camera (Lenzen et al. 2002), equipped with a 1024×1024 pixel Aladdin InSb array. Note that in May 2004, the CONICA detector was changed for a more efficient one. The coronagraphic masks used with NACO have diameters of $0.7''$. and $1.4''$. All NACO targets were observed in coronagraphy, using the CONICA Ks ($\lambda = 2.18 \mu\text{m}$, $\Delta\lambda = 0.35 \mu\text{m}$) filter. In direct imaging, we used the Bry ($\lambda = 2.166 \mu\text{m}$, $\Delta\lambda = 0.023 \mu\text{m}$) narrow band filter, as well as a neutral density filter, providing a transmissivity factor of 0.014, for the brightest stars. In order to correctly sample the PSF (better than Nyquist), we used the S27 objective, which gives a FoV of $28'' \times 28''$ centered on the stars.

The Θ_1 Ori C astrometric field (McCaughrean & Stauffer 1994) was observed (on November 12 2003, September 22 2004 and July 29 2005) to enable detector plate scale and orientation calibration. The orientation of true north of the S27 cam-

era was found respectively at -0.06° , 0.0° and -0.05° east of the vertical with an uncertainty of 0.20° and the plate scale was $27.01 \pm 0.05 \text{ mas/pix}$. On June 3 2003, the grade 2 astrometric calibration binary WDS21579-5500 from the Washington Visual Double Star Catalog (Worley & Douglass 1996) was observed and the S27 camera was found at $0.01 \pm 0.20^\circ$ east of the vertical. The plate scale remains stable at $27.01 \pm 0.05 \text{ mas}$.

2.3. Data reduction and analysis

The data were flat-fielded, sky subtracted and cross-correlated using the *eclipse* software (Devillard 1997). Companion candidates were identified using the “peak” *eclipse* algorithm. The relative positions between the companion candidates and the central star were determined using the deconvolution algorithm of Véran et al. (1998). These were double-checked using cross-correlation functions. The position of the parent star was measured on the direct image that followed the coronagraphic one. The shifts (≤ 1 pixel) induced between images taken in different filters have been accounted for. For NACO, these shifts were measured using a sequence of pinhole images recorded with the respective instrumental settings. For PUEO-KIR, direct images of a single star in narrow and broad band filters were recorded to determine them.

In order to estimate the relative flux between the star and any companion candidates, we used aperture photometry. The results for the two companions HD 1237 B and HD 27442 B are reported in Table 3. In the case of the close binary HD 196885, we used the myopic deconvolution algorithm *MISTRAL* (Conan et al. 2000) to obtain relative JHK photometry and relative astrometry (see Table 5). For HD 1237 and HD 27442, the transformation between the K_s filter of NACO and the K filter used by CTIO-2MASS was found to be negligible ($\leq 0.03 \text{ mag}$) with respect to uncertainties of our relative photometry. The detection limits were obtained, using the direct and the coronagraphic imaging data. The method consists of reducing the level of the PSF wing and in measuring the detection limit. For a given angular sector (typically 20 – 30°), centered on the star, we compute the azimuthal average of the PSF that we subtract from any angular direction in the sector. We then measure the 6σ detection limit, for a given radius from the star, in a sliding box of 5×5 pixels.

² These GTO runs were scheduled between May 21 and June 7 2003 (GTO-071.C-0507), on September 7 2003 (GTO-71.C-0462), and between November 11 and 17 2003 (GTO-072.C-0624). We also obtained open time observations on September 22 2004 (073.C-0468) and on July 28 and 29 2005 (075.C-0825).

³ <http://www.eso.org/instruments/naos/>

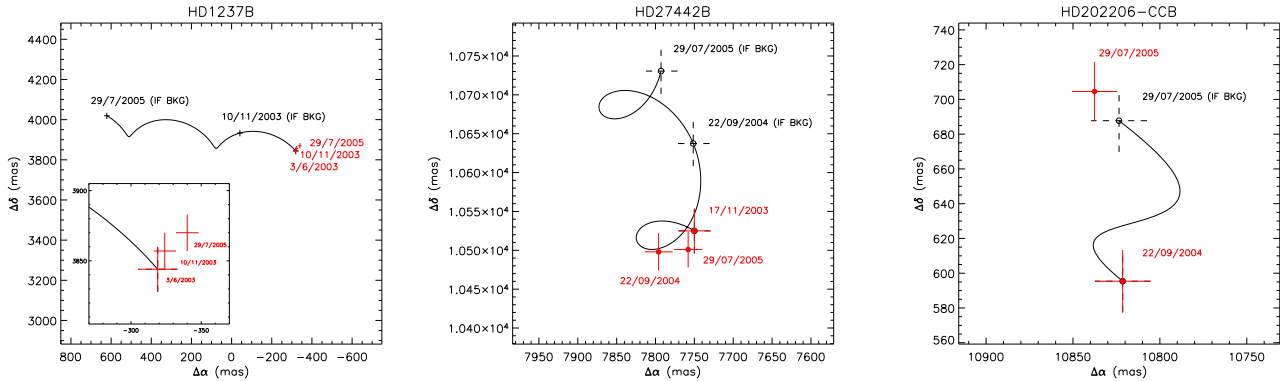


Fig. 2. VLT/NACO Measurements (*full circles* with uncertainties) of the offset positions of the companion HD 1237 B to A (*left*), of the companion HD 27442 B to A (*middle*) and of the companion candidate CC-B relative to HD 202206 (*right*). For each diagram, the expected variation of offset positions, if B is a background object, is shown (*solid line*), based on a distance and on a primary proper motion, as well as the initial offset position of B (or CC-B) from A. The *empty circles* give the corresponding expected offset positions of a background object for the different epochs of observations of HD 1237 A, HD 27442 A and HD 202206, with total uncertainties. In both cases, HD 1237 B and HD 27442 B are confirmed to be comoving objects. The candidate companion CC-B to HD 202206 has been rejected as comoving and is most likely a stationary background object. In addition, the NACO astrometric measurements clearly show an orbital motion of HD 1237 B relative to A, which confirms the companionship of this low mass star.

3. Results

3.1. Identification of companion candidates

We did not detect any companion candidates around the 6 stars HD 28185, HD 92788, HD 95128 (47 UMa), HD 106252, HD 186427 (16 Cyg B) and HD 217107. HD 95128 (47 UMa) and HD 186427 (16 Cyg B) had already been observed by Luhman & Jayawardhana (2002), using enhanced detection capabilities with the Keck II Telescope in conjunction with KCam (but with a search radius of 3.3"). They did not detect any fainter candidates.

Of the remaining 20 stars, at least one faint companion candidate was detected. The number of companion candidates and their status are summarized in Table 1.

- The stars HD 168443 and HD 187123 are in the line of sight of the galactic plane ($b < 15^\circ$) and several faint sources were detected. For HD 168443, we have detected more than 100 companion candidates among which 5 were identified by Luhman & Jayawardhana (2002) as background objects. For HD 187123, five companion candidates were detected including 2 identified by Luhman & Jayawardhana (2002). They all appear to be background objects.
- A faint companion candidate was detected for HD 89744 A. Using Sofi at the ESO New Technology Telescope, Mugrauer et al. (2004) identified this source as a background object. Although PUEO-KIR detection performances were better than Sofi, no additional faint companion candidates were detected. Note that a stellar companion exists around HD 89744 A, but at a larger separation than the KIR FoV (see Mugrauer et al. 2004).
- 8 stars (HD 52265, HD 114762, HD 121504, HD 141937, HD 154857 HD 162020, HD 179949 and HD 183263) have so far only been observed at one epoch. Additional follow-

up observations are needed to identify possible comoving companions.

- 6 other stars (HD 17051, HD 160691, HD 192263, HD 202206, in addition to the CFHT candidates HD 130322 and HD 187123) were found with companion candidates that happened to have different proper motions from their central stars. An example of the analysis of the proper and parallax motions is provided in Fig. 2 (*right*). We show respectively the expected offset positions and the observed offset positions of the companion candidate relative to HD 202206.
- Close to the star HD 196885, direct images reveal a close bright object (see Fig. 1). Eventhough we do not have second epoch measurements, the probability that this object is a background object is extremely small due to its proximity to the star HD 196885 and its relative brightness (see Table 5). Its status is detailed in Section 4.
- Finally, in 3 cases, the faint object shares a common proper motion with the central star: HD 1237, HD 13445 (Gl 86) and HD 27442 (see Fig. 1). Gl 86 B is a known companion (Els et al. 2001) and is mentioned just for completeness. HD 1237 B and HD 27442 B are bound companions (see Fig. 2). Astrometric measurements and photometric properties of the companions are summarized in Table 4 and 5. The results obtained for these two objects are discussed in Section 4.

3.2. Survey performances

The typical detection performances are reported in Table 2 for angular separations of 1 and 2". Using the K magnitude and the distance of the stars, we convert the typical contrast into absolute magnitude limit. Finally, based on the predictions of the BA98 (Baraffe et al. 1998) evolutionary model in the stellar

Table 3. Characteristics of the planetary hosts exhibiting additional linear RV trends.

Name	SpT	Age (Gyr)	M_A (M_\odot)	$M_{b, c \text{ sini}}$ (M_{Jup})	P (days)	e	RV drift ($\text{m.s}^{-1}.\text{yr}^{-1}$)	Ref.	ADDITIONAL COMPANION?	
									a_{min} (0.5 M_\odot) (AU)	a_{min} (0.1 M_\odot) (AU)
HD 28185	G5	5.5	1.0	5.7	383	0.07	11.0	1, 9, 10	≤ 6	≤ 25
HD 154187	G5	5.0	1.2	1.8	398	0.51	-14.0	2	≤ 15	≤ 70
HD 187123	G3V	5.0	1.0	0.48	3.096	0.43	-7.0	3, 4	≤ 8	≤ 40
HD 202206	G6V	5.0	1.15	17.4; 2.44	255.9; 1383.4	0.43; 0.267	42.9	5, 6	explained by the 2 nd planet	
HD 217107	G8IV	8.0	0.98	1.37; ≤ 13	7.1; ≥ 3000	0.13; ~ 0.5	38.0	7, 8	explained by the 2 nd planet	

REFERENCES: (1) Santos et al. 2001, (2) McCarthy et al. 2004, (3) Butler et al. 1998, (4) Vogt et al. 2000, (5) Udry et al. 2001, (6) Correia et al. 2005, (7) Fischer et al. 1999, (8) Vogt et al. 2005, (9) Schaefer et al. 1993, (10) Strassmeier et al. 2000

regime and the COND03 (Baraffe et al. 2003) model in the sub-stellar regime, the detection performances can be expressed in terms of mass for different ages: 0.5, 1.0, 5.0 and 10.0 Gyr. For stars as young as 0.5 Gyr, PUEO-KIR and NACO were sensitive to companions with masses down to 30 and 15 M_{Jup} respectively at 2". The individual detection limits for each planetary host are given in Fig. 3–9.

As expected, the VLT/NACO detection limits compare favourably to those obtained at Keck (Luhman & Jayawardhana 2002), despite the smaller aperture of the VLT. They also compare favourably with those obtained by Masciadri et al. (2005), using NACO. In both cases, the surveys were performed using saturated images, whereas our survey uses a coronagraph, which allows deeper observations. The comparison with the simultaneous differential imaging (SDI) technique is not straightforward as the detection limit with SDI does not uniquely translate into a detection limit in terms of contrast and, thus temperature and mass. Close to the star, the detected signal is actually the subtraction of two narrow band images centered inside and outside the CH_4 signature. A comparison of the NACO coronagraph detection limit to the SDI one, taking into account the *effective* flux that remains after subtraction, shows that, when scaled to similar exposure times, the SDI does not provide a significant gain in the domain accessible to the coronagraph images ($\geq 0.35''$). Inside this region, given the NACO PSF, the 5 Gyr-old objects that we can expect to detect mainly have greater temperatures than 1200 K. Therefore, their spectra present no significant CH_4 absorption at SDI bands.

4. Discussion

4.1. Stars with drifts and undetected companions

The 6 stars HD 13445 (G186) HD 28185, HD 154857, HD 187123, HD 202206 and HD 217107 exhibit a long term RV drift, possibly indicating the presence of long-period companions. The case of HD 13445 (G186) is discussed in another paper (Lagrange et al. 2006). The properties of the 5 other planetary systems are reported in Table 3.

For the 3 systems HD 28185, HD 154857 and HD 187123, we assume, for a rough estimation, that the outer companion, responsible for the RV long term drift, evolves on a circular orbit with a mass negligible compared to the primary

($M_3 < 0.1 M_\odot$). If so, the RV data enable us to exclude a domain of mass as a function of the semi-major axis (see shadowed zones in Fig. 7, 9, 11). Considering now our imaging data, we know that no comoving companion candidates were detected for the 2 stars HD 28185 and HD 187123. However, contrary to the RV measurements, the imaging data do not allow us to rule out definitively a domain of mass and semi-major axis. Imaging is indeed only sensitive to projected physical separations. We can only assert that, although we were sensitive down to given minimum semi-major axis (see Table 3 for masses of 0.1 and 0.5 M_\odot), we did not detect any comoving objects that could explain the long term RV drifts of the central stars. In the case of HD 154857 observed at one epoch, several companion candidates have been detected and future follow-up observations are needed to confirm if they are comoving and if they could be responsible for the drift.

For the two systems HD 202206 and HD 217107, recent RV measurements have explained the existence of the long term drift with the detection of a third body in the system. For HD 202206, Correia et al. (2005) showed that the RV drift is caused by a lower mass planet, clearly beyond the detection performances of our imaging survey. In the case of HD 217107, Vogt et al. (2005) identified a significant curvature in the velocities suggesting the existence of a second possible planet, HD 217107 c, likely orbiting at 3–8 AU. Our non detection supports the fact that HD 217107 c, is unlikely to be a stellar companion.

4.2. A K-dwarf companion to HD 196885?

HD 196885 A is a F8IV star, part of a wide binary system with the star BD+104351 B located $\sim 190''$ North of HD 196885 A. HD 196885 A is also known to host a planet (hereafter HD 196885 Ab), detected through RV measurements during the Lick RV survey. Although no related publications can be found, the EGP characteristics are reported by the California & Carnegie Planet Search Team on their webpage⁴. HD 196885 Ab has a minimum mass of $M_2 \sin i = 1.84 M_{\text{Jup}}$, a period $P = 386.0$ days and an eccentricity $e = 0.3$. In addition, at about 0.7" from HD 196885 A, we have imaged a relatively bright companion candidate (see in Table 3). Based

⁴ <http://exoplanets.org/esp/hd196885/hd196885.shtml>

Table 4. Offset positions of the HD 1237 B and HD 27442 B relative to the parent stars.

Name	UT Date	OBSERVED				IF BACKGROUND		χ^2	P(χ^2)
		$\Delta\alpha$ (mas)	$\Delta\delta$ (mas)	Separation (mas)	PA ($^\circ$)	$\Delta\alpha$ (IF BKG) (mas)	$\Delta\delta$ (IF BKG) (mas)		
HD 1237 B	03/06/2003	-319 ± 14	3844 ± 16	3857 ± 15	355.3 ± 0.3				
	10/11/2003	-324 ± 8	3857 ± 13	3871 ± 11	355.1 ± 0.2	-41 ± 14	3933 ± 17	290	$< 1e-9$
	29/07/2005	-340 ± 8	3870 ± 13	3885 ± 15	354.9 ± 0.3	621 ± 14	4019 ± 16	3500	$< 1e-9$
HD 27442 B	17/11/2003	7750 ± 21	10525 ± 29	13070 ± 21	36.3 ± 0.2				
	22/09/2004	7796 ± 18	10498 ± 24	13076 ± 21	36.6 ± 0.2	7751 ± 21	10637 ± 29	17	$3e-4$
	29/07/2005	7758 ± 18	10501 ± 23	13056 ± 21	36.4 ± 0.2	7793 ± 21	10739 ± 29	39	$6e-8$

on the 2MASS catalog (Cutri et al. 2003) and the photometry of HD 196885 B, we can estimate the probability of finding HD 196885 B within $3''$ of the line of sight of HD 196885 A. Within a field of $5 \times 5 \text{ deg}^2$, centered around HD 196885 A, the density of nIR sources of similar JK magnitudes than HD 196885 B is about $19.3 \text{ sources/deg}^2$. The probability of detecting HD 196885 B within a radius of $3''$ of A is then $\sim 1e-5$, therefore HD 196885 B is unlikely to be a background source.

At a distance of 33 pc measured for HD 196885 A (Perryman et al. 1997), the JHK absolute photometry of the visual companion HD 196885 B would be: $M_J = 9.8 \pm 0.2$, $M_H = 9.2 \pm 0.2$ and $M_K = 8.7 \pm 0.2$. Using BA98 model predictions, we derive a possible mass for HD 196885 B of $0.6 M_\odot$, using an age estimate for the system of 0.5 Gyr (Lambert et al. 2004). Therefore, HD 196885 B is likely to be a late-K dwarf orbiting HD 196885 A at a projected physical distance of 25 AU. With an estimated period of $\sim 90 \text{ yr}$, we should be able to monitor the orbital motion of B relative to A. Using RV measurements, this will enable us to determine the orbital characteristics of the system and to test how the inner planetary system has been affected by this massive stellar companion. Presently, the planet HD 196885 Ab does not show unusual physical properties that could be explained by the presence of HD 196885 B. The maximum drift per year, induced by an outer companion of $0.6 M_\odot$ on the $1.3 M_\odot$ star HD 196885 A, is about $110 \text{ m.s}^{-1} \cdot \text{yr}^{-1}$ (assuming a circular orbit). Therefore, the influence of HD 196885 B should be clearly observed on the RV curve of HD 196885 A.

4.3. An M-dwarf companion to HD 1237

HD 1237 A is a bright G6V dwarf with a space velocity vector, a Lithium abundance and chromospheric activity which indicate that this star is likely a member of the 0.8 Gyr old Super Cluster of the Hyades (see Naef et al. 2001). In the course of the CORALIE RV survey, Naef et al. (2001) discovered a possible substellar companion (hereafter HD 1237 Ab), with a minimum mass of $M_2 \sin i = 1.94 M_{\text{Jup}}$, a period $P = 311.29 \text{ days}$ and an eccentricity $e = 0.24$.

The companion HD 1237 B has been imaged at a projected physical separation of 68 AU from HD 1237 A. Fig. 2 displays, in a ($\Delta\alpha$, $\Delta\delta$) diagram, the offset positions of HD 1237 B from A, observed at 3 different epochs. The expected evolution of the relative A-B positions, under the assumption that B is a station-

Table 5. Photometry of the 3 systems HD 1237 AB, HD 27442 AB and HD 196885 AB.

Component	J (mag)	H (mag)	Ks (mag)
HD 1237 A ^a	5.37 ± 0.03	4.99 ± 0.04	4.86 ± 0.03
HD 1237 B ^b	11.0 ± 0.2	10.4 ± 0.2	9.9 ± 0.2
HD 27442 A ^a	2.4 ± 0.2		1.8 ± 0.2
HD 27442 B ^b	13.0 ± 0.3		12.5 ± 0.2
HD 196885 A ^b	5.5 ± 0.1	5.2 ± 0.1	5.1 ± 0.1
HD 196885 B ^b	9.1 ± 0.1	8.5 ± 0.1	8.2 ± 0.1

^a from the 2MASS All-Sky Catalog of Point Sources (Cutri et al. 2003).

^b from ^a and NACO measurements presented in this work.

nary background object, is indicated in Fig. 2 and in Table 4. With a normalized probability $P(\chi^2) < 1e-9$ that HD 1237 B is a background stationary object, we find that HD 1237 A and B are comoving. At a distance of 17.6 pc (Perryman et al. 1997), the JHK absolute photometry of the comoving companion HD 1237 B is: $M_J = 9.8 \pm 0.2$, $M_H = 9.2 \pm 0.2$ and $M_K = 8.7 \pm 0.2$. By comparison with the predictions of the BA98 model, we derive a possible mass of $0.13 M_\odot$ for an age of 0.8 Gyr. This implies that HD 1237 B is likely a mid-M dwarf. Moreover, our astrometric observations marginally reveal an orbital motion of HD 1237 B relative to A (see Fig. 2). Additional observations, coupled to RV measurements, should enable us to derive the orbital properties of HD 1237 B and to investigate whether HD 1237 B has affected the dynamics of the planet HD 1237 Ab. As for the HD 196885 system, the planet HD 1237 Ab does not show any unusual physical properties which could be caused by HD 1237 B. The maximum drift per year that should produce HD 1237 B on A is $4 \text{ m.s}^{-1} \cdot \text{yr}^{-1}$ (assuming a circular orbit). This presence of this drift will only be detectable on a period of several years since the chromospheric activity of HD 1237 A induces a RV residual of 18 m s^{-1} , which dominates the RV measurements.

4.4. A possible white dwarf orbiting HD 27442?

HD 27442 A is a K2IV subgiant star with an age estimate of 10 Gyr (Randich et al. 1999). In the course of the Anglo-

Australian RV survey, Butler et al. (2001) have detected a giant planet (hereafter HD 27442 Ab) to the star HD 27442 A. HD 27442 Ab has a minimum mass of $M_{2\text{sini}} = 1.28 M_{\text{Jup}}$ and orbits around HD 27442 A with a period $P = 423.84$ days and with an eccentricity $e = 0.07$.

At $\sim 13''$ (240 AU in projected physical separation) from HD 27442 A, we have detected the faint comoving companion HD 27442 B. The normalized probability that HD 27442 B is a background star (see Fig. 2 and Table 4) is $P(\chi^2) < 1e - 7$. At 18.2 pc (Perryman et al. 1997), we derive a JK absolute photometry for HD 27442 B: $M_J = 11.7 \pm 0.2$ and $M_K = 11.2 \pm 0.2$. The position of HD 27442 B coincides with that of a $V = 12.5$ source, reported in year 1930 in the Washington Visual Double Star Catalog (WDS, Worley & Douglass 1997) at a relative position of $\Delta = 13.7''$ and $PA = 35^\circ$ from HD 27442 A. We have probably detected the nIR counterpart of this object. To test this hypothesis, we can examine the point where HD 27442 B would be expected to appear if it had been a background source. Based on the relative position of B from A in year 1930 and the proper motion of HD 27442 A, we find that this background source would be located at $11.4''$ East and $23.5''$ North from HD 27442 A. We do not detect any object at such a position in any catalogs or using NTT/Sofi H-band images from the ESO archive. This null detection supports the interpretation that both observations correspond to the same object.

The visible and nIR photometry of HD 27442 B appears incompatible with that expected for any main sequence stars or brown dwarfs at 18.2 pc. This photometry is however consistent with that predicted by the evolutionary model of Bergeron et al. (2001) for white dwarfs with hydrogen- and helium-rich atmospheres. HD 27442 B is then most likely to be a white dwarf companion with a mass ranging between 0.3 and $1.2 M_\odot$ and an effective temperature ranging between 9000 and 17000 K. If confirmed, this system would be a similar case to HD 13445 (G186) AB. G186 A is indeed a K0V star hosting a $4 M_{\text{Jup}}$ (minimum mass) planet and a probable $0.5 M_\odot$ white dwarf companion orbiting at about 20 AU. Given a minimum separation of ~ 240 AU between HD 27442 A and B, it is very unlikely that the latter influenced the dynamics of the inner planetary system. The maximum drift induced by a possible 0.3 - $1.2 M_\odot$ outer companion on the $1.2 M_\odot$ star HD 27442 A is less than $2 \text{ m.s}^{-1} \cdot \text{yr}^{-1}$ (assuming a circular orbit). Improved detection capabilities and RV measurements over several years are required in order to detect the presence of HD 27442 B in the RV curve of A.

5. Conclusions

We have conducted a deep coronagraphic adaptive optics imaging survey of 26 stars with planets detected through radial velocity measurements. The domain investigated typically ranges between $0.1''$ to $15''$ (i.e. about 3 to 500 AU, according to the mean distance of the sample). The survey is sensitive to stellar and substellar companions with masses greater than $30 M_{\text{Jup}}$ (0.5 Gyr) with CFHT and $15 M_{\text{Jup}}$ (0.5 Gyr) with VLT, at $2''$ (~ 60 AU) from the primary star. The main results are that:

- 6 stars did not show any companion candidates: HD 28185, HD 92788, HD 95128 (47 UMa), HD 106252, HD 186427 (16 Cyg B) and HD 217107,
- 8 stars were surrounded by faint sources all identified as background, stationary, objects: HD 17051, HD 89744, HD 130322, HD 160601, HD 168443, HD 187123, HD 192263 and HD 202206,
- 3 stars revealed comoving objects which are likely companions: HD 1237, HD 13445 (G186) and HD 27442. Orbital motion are detected for the companions to HD 13445 (G186) and to HD 1237, confirming the companionship of both objects. A close and bright stellar companion candidate is also detected to the star HD 196885 with a probability for this object to be a background object which is very low,
- 8 stars revealed at least one faint companion candidate. These require follow-up observations to identify possible comoving companions. They are: HD 52265, HD 114762, HD 121504, HD 141937, HD 154857, HD 162020, HD 179949 and HD 183263.

The five stars HD 28185, HD 154857, HD 187123, HD 202206 and HD 217107 exhibit a long trend RV drift. The companion to HD 13445 (G186) is a known physical companion, discussed in more detail in a forthcoming paper (Lagrange et al. 2006). The companions HD 1237 B and HD 196885 B are likely a mid-M dwarf and a late-K dwarf, based on a comparison of their photometry with evolutionary model predictions. Future spectroscopic observations should enable us to confirm the low stellar mass status of both objects. In addition, a dedicated monitoring of their orbital motion, to complement RV measurements, should enable us to derive the orbital parameters of these systems and investigate if these companions have affected the dynamics of the inner planetary systems. Finally, we also found that the comoving companion HD 27442 B is likely a white dwarf companion orbiting the 10 Gyr-old subgiant HD 27442 A. This would mean that this system would be very similar to the binary system HD 13445 (G186) AB, with a primary which is a planetary host and the secondary, a $0.5 M_\odot$ white dwarf located at ~ 20 AU. Future spectroscopic observations are required to confirm this scenario.

Acknowledgements. We would like to thank the staff of ESO-VLT and CFHT and Gilles Chabrier, Isabelle Baraffe and France Allard for providing the latest update of their evolutionary models. We also acknowledge partial financial support from the *Programmes Nationaux de Planétologie et de Physique Stellaire* (PNP & PNPS), in France.

References

- Baraffe I., Chabrier G., Allard F. & Hauschildt P.H., 1998, A&A, 337, 403
- Baraffe I., Chabrier G., Barman T.S., Allard F. & Hauschildt P.H. 2003, A&A, 402, 701
- Becklin E.E. & Zuckerman B. 1988, Nature, 336, 656
- Bergeron P., Leggett S.K., & Ruiz M.T. 2001, ApJS, 133, 413
- Beuzit J.-L., Sgransan D., Forveille T. et al. 2004, A&A, 424, 997

- Butler R.P. & Marcy G.W. 1996, *ApJ*, 533, L147
- Butler R.P., Marcy G.W., Vogt S.S. & Apps K. 1998, *PASP*, 110, 1389
- Butler R.P., Vogt S.S., Fischer D. et al. 2000, *ApJ*, 545, 504
- Butler R.P., Tinney C.G., Marcy G.W. et al. 2001, *ApJ*, 555, 410
- Chauvin G., Thomson M., Dumas C. et al. 2003, *A&A*, 404, 157
- Chauvin G., Lagrange A.-M., Dumas C. et al. 2004, *A&A*, 425, L25
- Chauvin G., Lagrange A.-M., Lacombe F. et al. 2005, *A&A*, 430, 1027
- Chauvin G., Lagrange A.-M., Zuckerman B. et al. 2005, *A&A*, 438, L29
- Conan, J.-M., Fusco, T., Mugnier, L. et al. 2000, *SPIE*, Vol. 4007
- Cochran W., Hatzes A., Butler P. & Marcy G. 1997, *ApJ*, 483, 457
- Correia S., Udry S., Mayor M. et al. 2005, *A&A*, 440, 751
- Devillar N. 1997, *The messenger*, 87
- Eggenberger A., Udry S. & Mayor M. 2004, *A&A*, 417, 513
- Els S.G., Sterzik M.F., Marchis F. et al. 2001, *A&A*, 370, L1
- Fischer D.A., Marcy G.W., Butler R.P. et al. 1998, *PASP*, 111, 50
- Fischer D.A., Marcy G.W., Butler R.P. et al. 2000, *ApJ*, 551, 1107
- Fischer D.A., Marcy G.W., Butler R.P. et al. 2001, *ApJ*, 564, 1028
- Fischer D.A., Marcy G.W., Butler R.P. et al. 2002, *PASP*, 114, 529
- Forveille T., Sgransan D., Delorme P. et al. 2004, *A&A*, 427, L1
- Gizis J.E., Kirkpatrick J.D., Burgasser A. et al. 2001, *ApJ*, 551, L163
- Korzennik S., Brown T., Fischer D., Nisenson P. & Noyes R. 2000, *ApJ*, 533, L147
- Kurster M., Endl M., Els S., Hatzes A. et al. 2000, *A&A*, 353, L33
- Lagrange A.-M., Beust H., Udry S. et al. 2006, *A&A*, accepted
- Latham D.W., Stefanik R.P., Mazeh T., Mayor M. & Burki G. 1989, *Nature*, 339, 38
- Lenzen, R., Hofmann, R., Bizenberger, P. & Tusche, A., 1998, *SPIE*, Vol. 3354
- Liu M.C., Fischer D.A., Graham J.R. et al. 2002, *ApJ*, 571, 519
- Lowrance, P. J., McCarthy, C., Becklin, E. E. et al. 1999, *ApJ*, 512, L69
- Lowrance, P. J., Schneider, G., Kirkpatrick, J. et al. 2000, *ApJ*, 541, L390
- Luhman, K. & Jayawardhana, R. 2002, *ApJ*, 566, 1132
- Marcy G., Butler R.P., Vogt S.S. et al. 2005, *ApJ*, 619, 570
- Masciadri E., Mundt R., Henning Th., Alvarez C. & Barrado y Navascués D. 2005, *ApJ*, 625, 1004
- Mayor, M. & Queloz, D. 1995, *Nature* 378, 355
- Mayor M., Udry S., Naef D. et al. 2004, *A&A*, 415, 391
- McCaughrean M.J. & Stauffer J.R. 1994, *AJ*, 108, 1382
- McCarthy, C. & Zuckerman, B. 2004, *AJ*, 127, 2871
- McCarthy C., Butler R.P., Tinney C.G. et al. *ApJ*, 617, 575
- Metchev S.A. & Hillenbrand L.A. 2004, *ApJ*, 617, 1330
- Mugrauer M & Neuhäuser R., 2005, *MNRAS*, 361, 15
- Mugrauer M, Neuhäuser R., Mazeh, T., Guenther E. & Fernández, M. 2004, *AN*, 325, 718
- Naef D., Mayor M., Pepe F. et al. 2001, *A&A* 375, 205
- Nakajima T., Oppenheimer B.R., Kulkarni S.R. et al. 1995, *Nature* 378, 463
- Oppenheimer B.R., Golimowski D.A., Kulkarni S.R. et al. 2001, *AJ*, 121, 2189
- Patience J., White R.J., Ghez, A. M. et al. 2002, *ApJ*, 581, 654
- Perryman M.A.C., Lindegren L., Kovalevsky J. et al. 1997, *A&A*, 323, 49
- Potter D., Martn E.L., Cushing M.C. et al. 2002, *ApJ*, 567, 133
- Queloz D., Mayor M., Weber L. et al. 2000, *A&A*, 354, 99
- Randich S., Gratton R., Pallavicini R., Pasquini L. & Carretta E. 1999, *A&A*, 348, 487
- Rivera & Lissauer, 2000, *ApJ*, 530, 454
- Rousset G., Lacombe F., Puget P. et al., 2002, *SPIE*, Vol. 4007
- Santos N.C., Mayor M., Naef D. et al. 1999, *A&A*, 356, 599
- Santos N.C., Mayor M., Naef D., Pepe F. et al. 2001, *A&A*, 379, 999
- Santos N.C., Bouchy F., Mayor M. et al. 2004, *A&A*, 426, L19
- Schaerer D., Charbonnel C., Meynet G., Maeder A. & Schaller G. 1993, *A&AS*, 102, 339
- Strassmeier K.G., Washuettl A., Granzer T., Scheck M. & Weber M. 2000, *A&AS*, 142, 275
- Tinney C., Butler P., Marcy G. et al. 2000, *ApJ*, 551, 507
- Udry S., Mayor M., Naef D. et al. 2000, *A&A*, 356, 590
- Udry S., Mayor M., Clausen J.V. et al. 2003, *A&A*, 407, 369
- Vogt S.S., Marcy G.W., Butler R.P., Apps K. 2000, *ApJ*, 536, 902
- Vogt S.S., Butler P.R., Marcy G.W. et al. 2005, *ApJ*, 632, 638
- Worley C. E. & Douglass G. G. 1997, *A&AS*, 125, 123

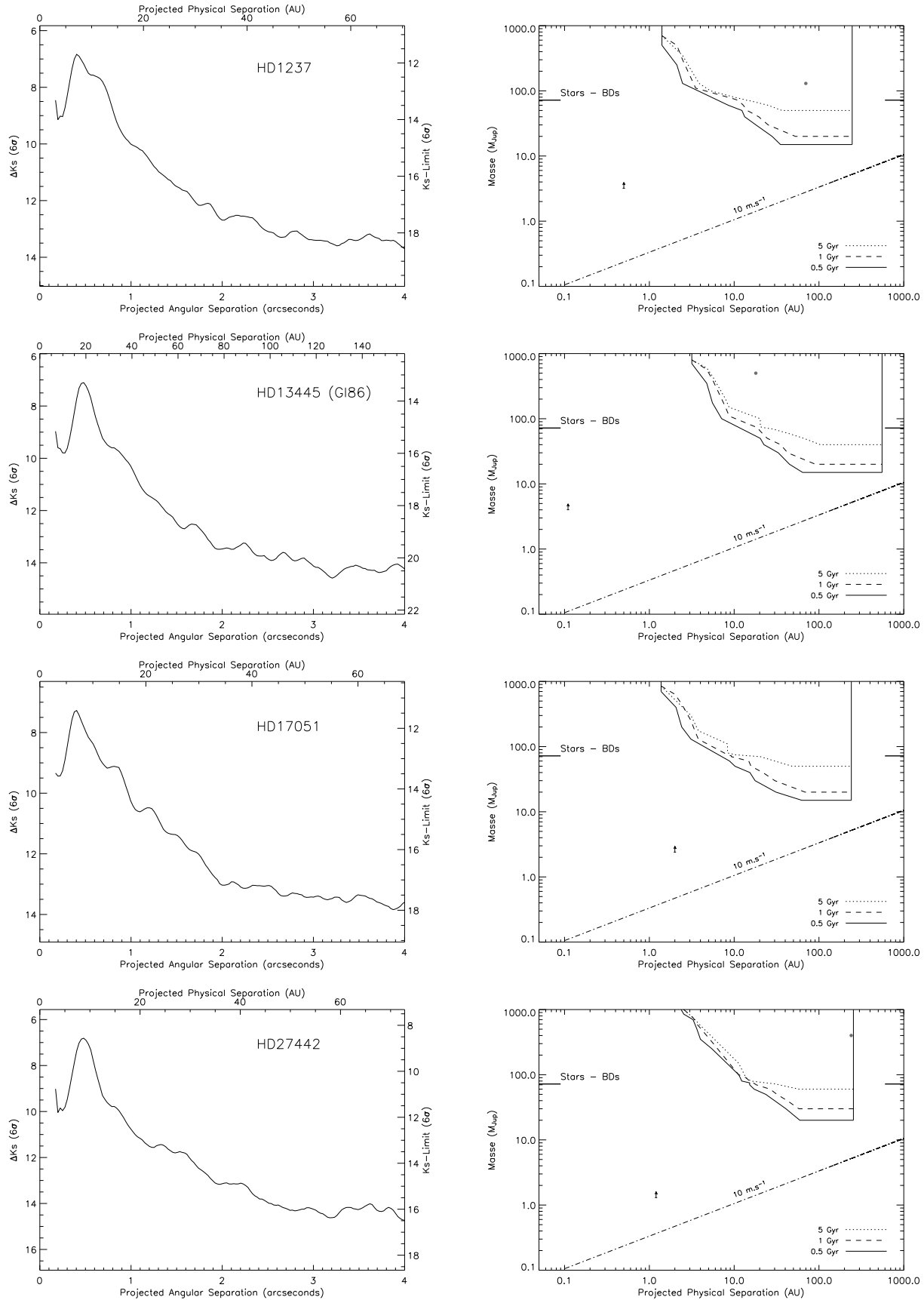


Fig. 3. Detection Limits of HD 1237 (November 2003, VLT/NACO, total exposure time of 300s), HD 13445 (Gl 86) (July 2005, VLT/NACO total exposure time of 270s), HD 17051 (November 2003, VLT/NACO total exposure time of 360s) and HD 27442 (July 2005, VLT/NACO total exposure time of 105s). See detail of the detection limit estimation in Section 2.2

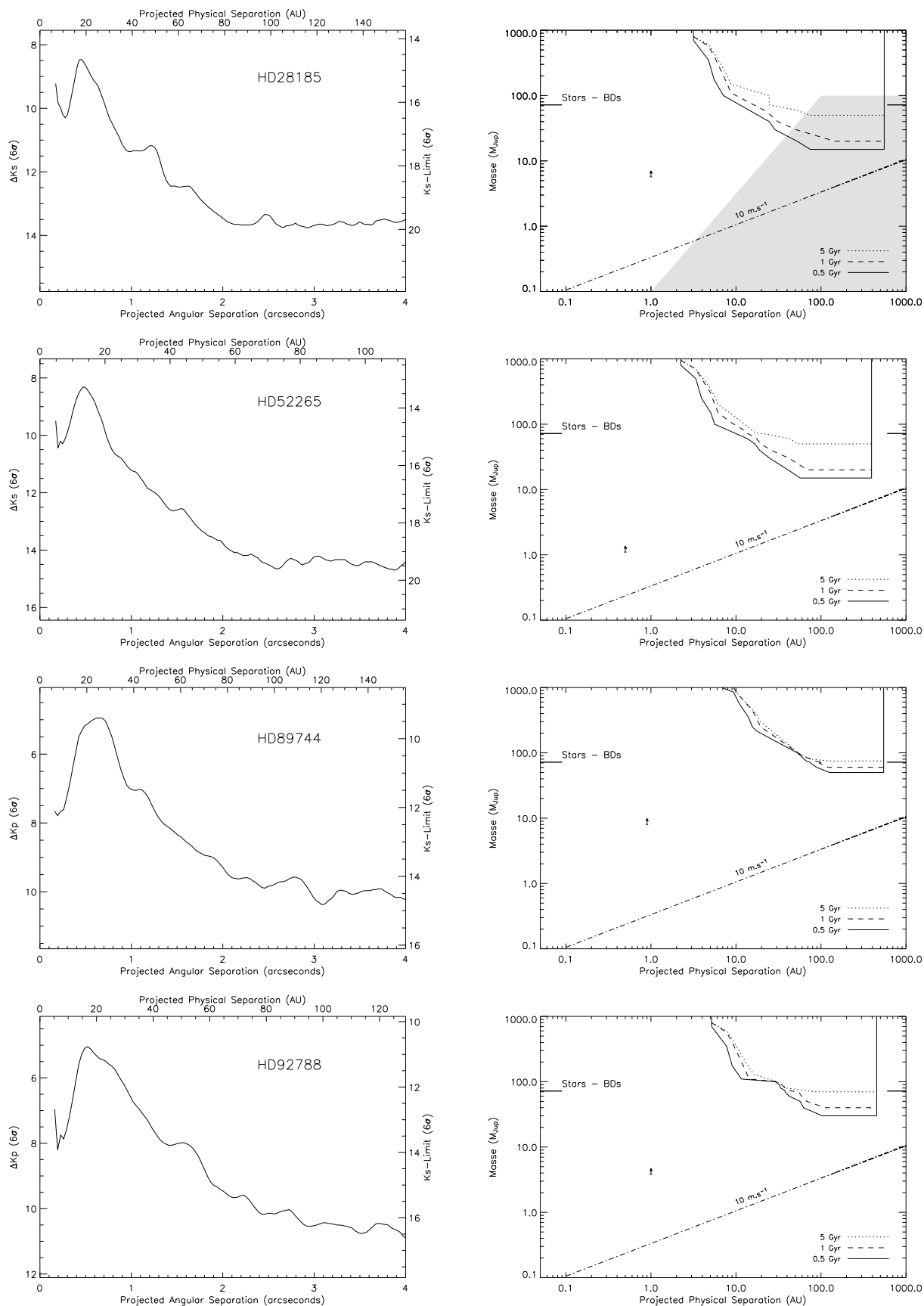


Fig. 4. Detection Limits of HD 28185 (July 2005, VLT/NACO, total exposure time of 160s), HD 52265 (November 2003 VLT/NACO, total exposure time of 300s), HD 89744 (May 2003, CFHT/PUEO-KIR, total exposure time of 200s) and HD 92788 (May 2003, CFHT/PUEO-KIR, total exposure time of 300s). See detail of the detection limit estimation in Section 2.2

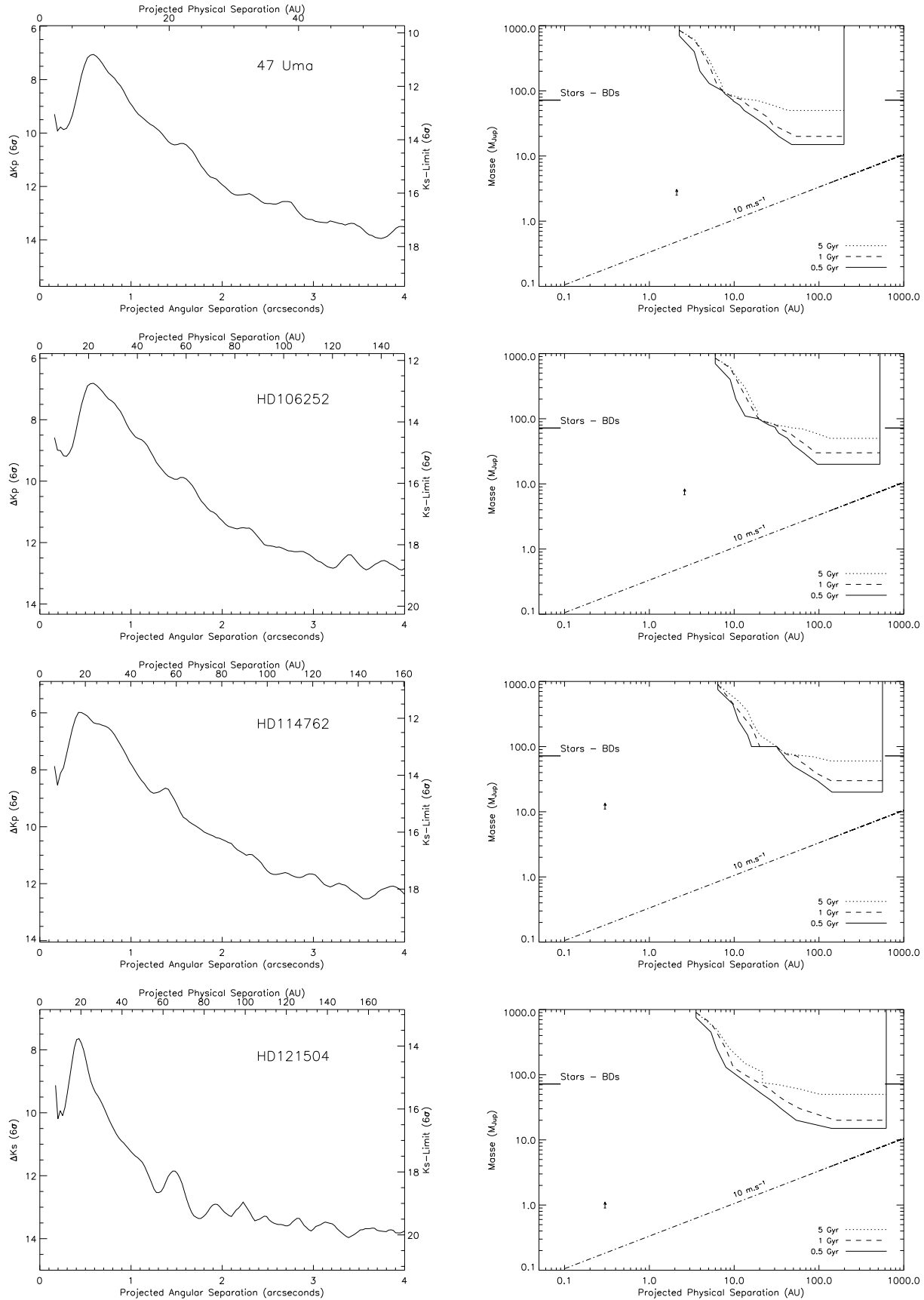


Fig. 5. Detection Limits of HD 95128 (47 Uma) (May 2003, CFHT/PUEO-KIR, total exposure time of 140s), HD 106252 (May 2003, CFHT/PUEO-KIR, total exposure time of 300s) and HD 114762 (May 2003, CFHT/PUEO-KIR, total exposure time of 300s) and HD 121504 (July 2005, VLT/NACO, total exposure time of 300s). See detail of the detection limit estimation in Section

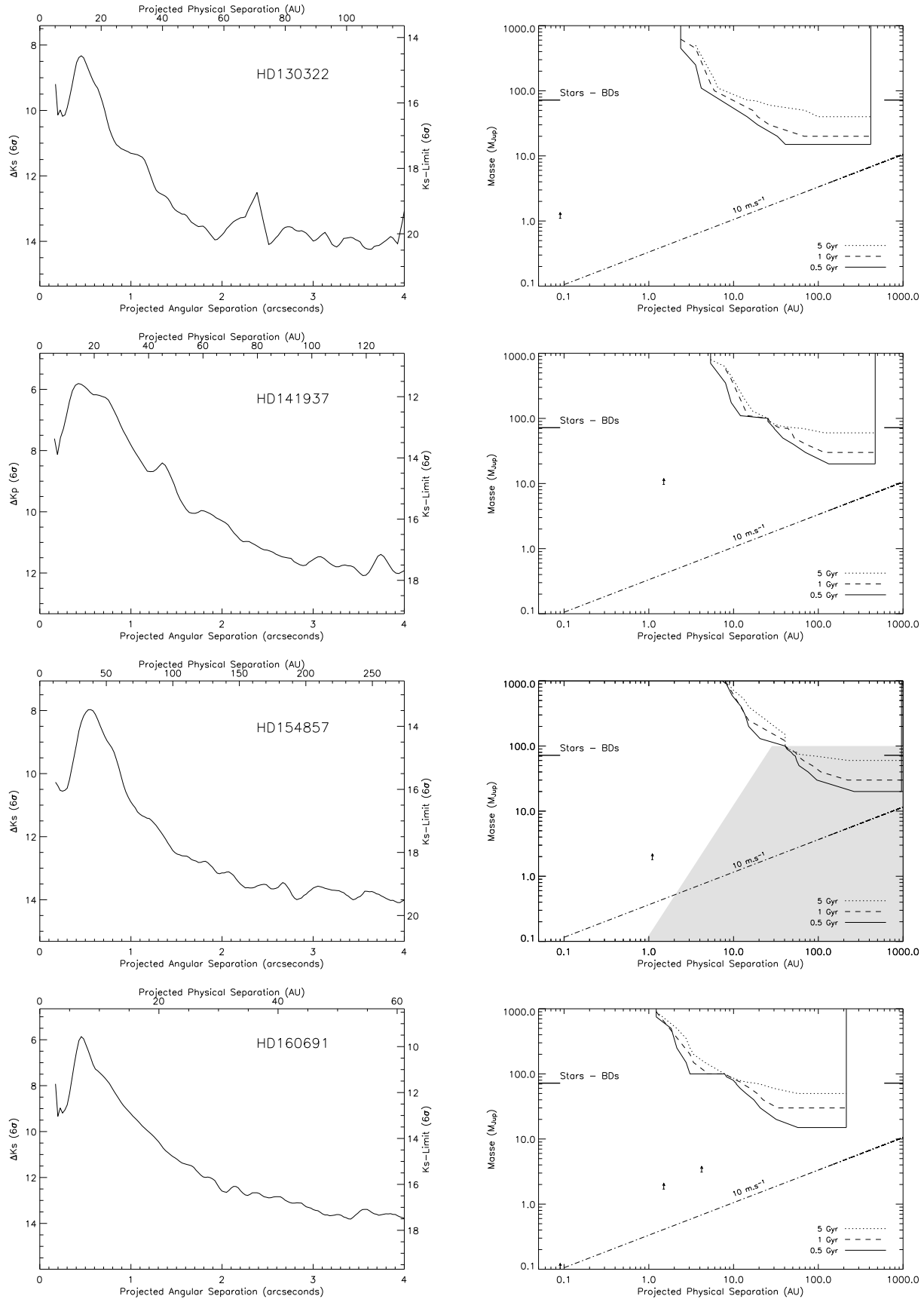


Fig. 6. Detection Limits of HD 130322 (July 2005, VLT/NACO, total exposure time of 300s), HD 141937 (May 2003, CFHT/PUEO-KIR, total exposure time of 200s), HD 154857 (July 2005, VLT/NACO, total exposure time of 300s) and HD 160691 (July 2005, VLT/NACO, total exposure time of 240s). See detail of the detection limit estimation in Section 2.2

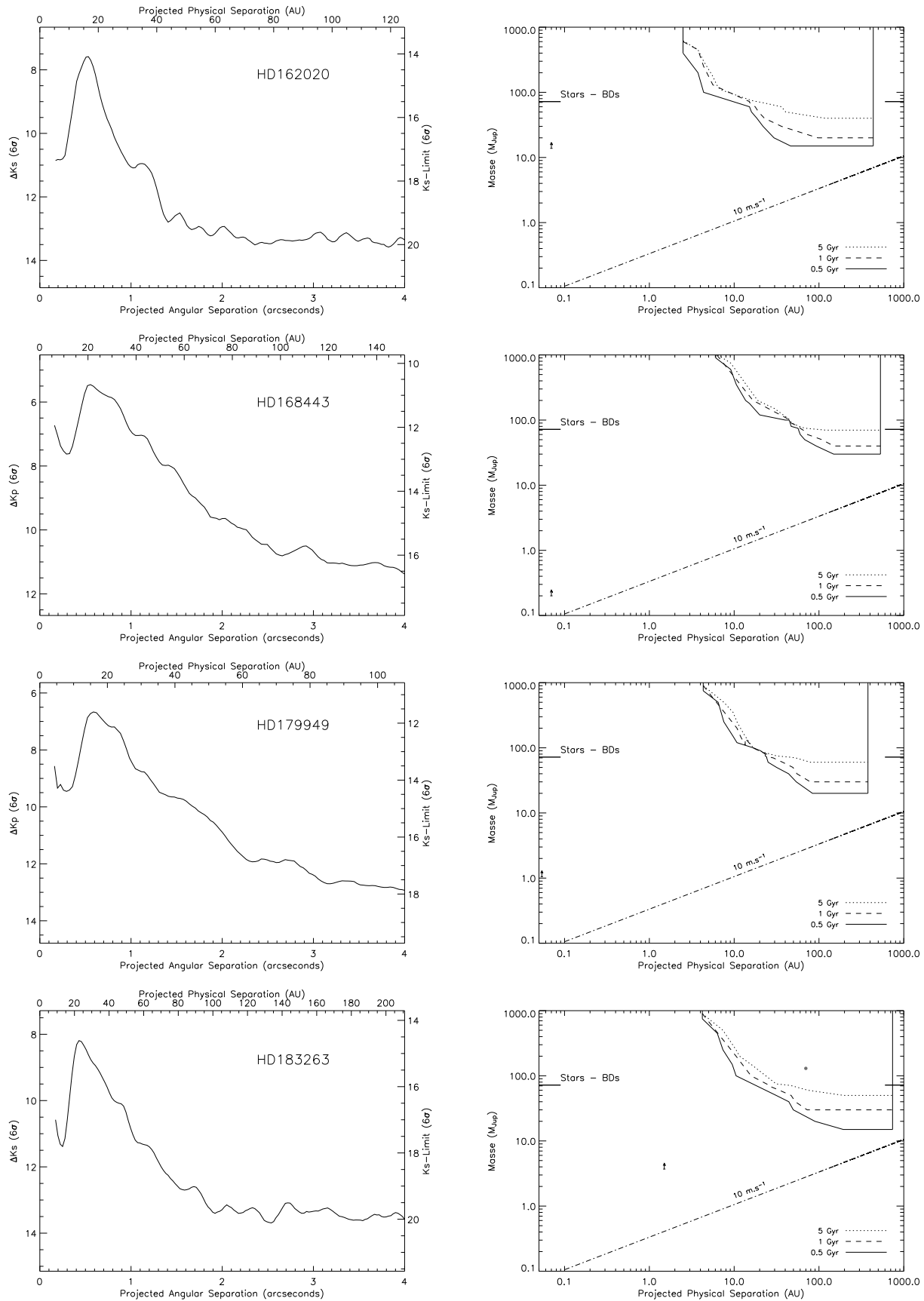


Fig. 7. Detection Limits of HD 162020 (July 2005, VLT/NACO, total exposure time of 300s), HD 168443 (May 2003, CFHT/PUEO-KIR, total exposure time of 300s), HD 179949 (November 2003, CFHT/PUEO-KIR, total exposure time of 300s) and HD 183263 (July 2005, VLT/NACO, total exposure time of 300s). See detail of the detection limit estimation in Section 2.2

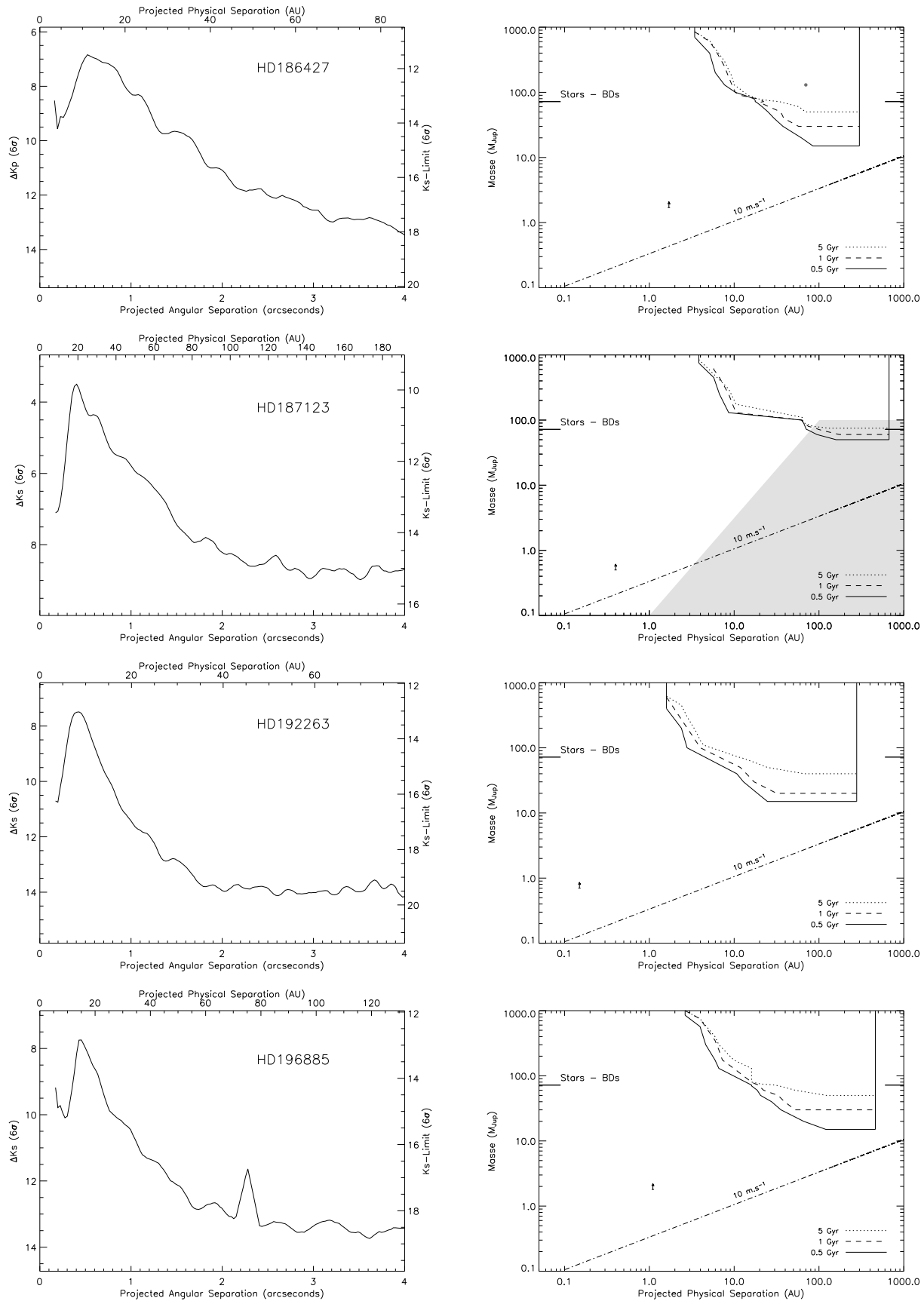


Fig. 8. Detection Limits of HD 186123 or 16 Cyg B (May 2003, CFHT/PUEO-KIR, total exposure time of 204s), HD 187123 (July 2005, VLT/NACO, total exposure time of 49s), HD 192263 (November 2003, VLT/NACO, total exposure time of 375s) and HD 196885 (July 2005, VLT/NACO, total exposure time of 300s). See detail of the detection limit estimation in Section 2.2

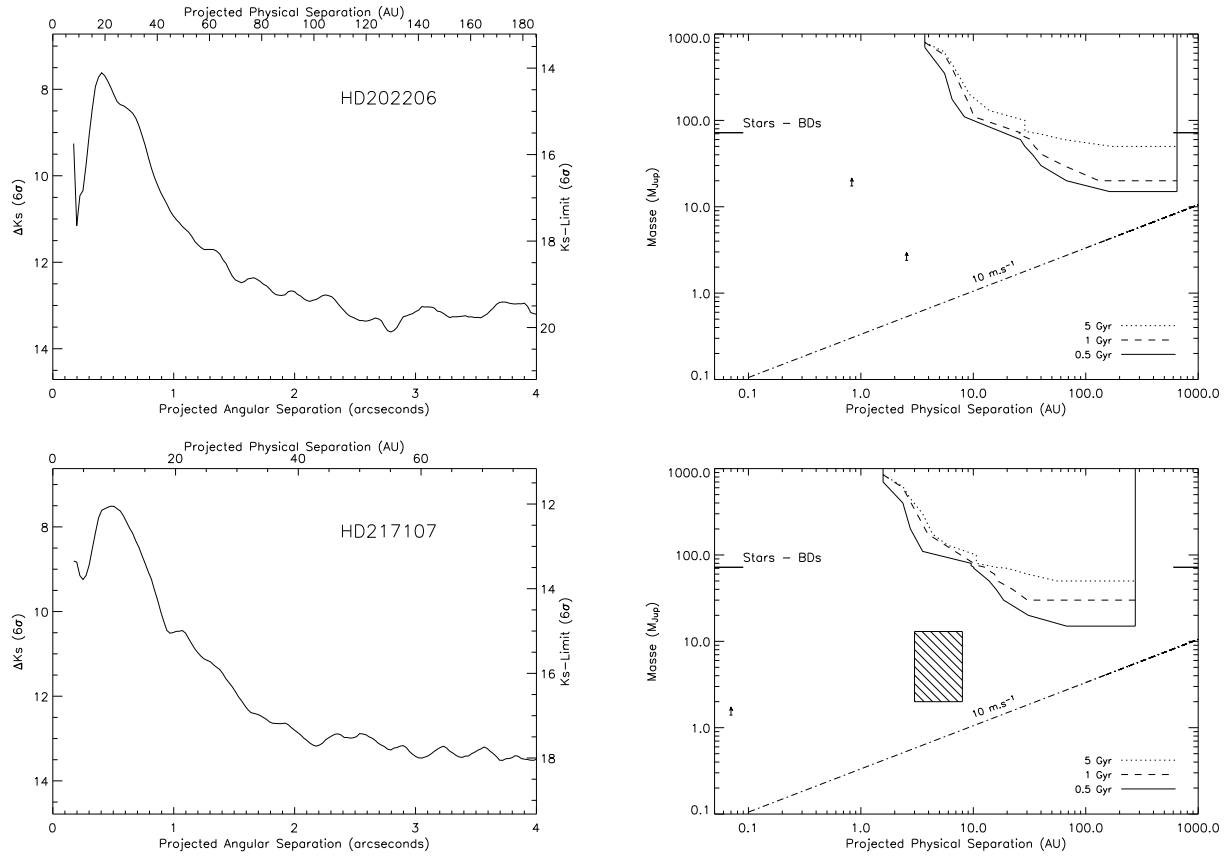


Fig. 9. Detection Limits of HD202206 (July 2005, VLT/NACO, total exposure time of 300s) and HD217107 (July 2005, VLT/NACO, total exposure time of 228s). See detail of the detection limit estimation in Section 2.2. On the detection limit of HD217107, converted in mass, the *dashed box* give the result of the best-fit orbit from (Vogt et al. 2005), which strongly suggests that the third component HD 217107c has an orbit of 3–8 AU and a mass within the planetary regime (less than $13 M_{\text{Jup}}$) rather than stellar or brown dwarf.

